Physica E ▮ (▮▮▮▮) ▮▮▮–▮▮▮

Contents lists available at SciVerse ScienceDirect

Physica E

journal homepage: www.elsevier.com/locate/physe

Fabrication and optical properties of porous InP structures

A.V. Atrashchenko [a], V.N. Katz [a], V.P. Ulin [a], V.P. Evtikhiev [a], V.P. Kochereshko [a,b,*]

[a] Ioffe Physical-Technical Institute, Russian Academy of Sciences, Politekhnicheskaya ul. 26, St. Petersburg 194021, Russia
[b] Spin-Optics Laboratory, St. Petersburg State University, Ulyanovskaya 1, Peterhof, St. Petersburg 198504, Russia

ARTICLE INFO

Article history:
Received 9 December 2011
Received in revised form
30 January 2012
Accepted 10 February 2012

ABSTRACT

Technology for the fabrication of a homogeneous array of pores in an A3B5 semiconductor matrix has been developed. Characterization with Scanning Electron Microscope and optical characterization of these samples have been carried out. Refractive indexes for the light polarized along and perpendicular to the pores have been measured. We have found that the measured values of the refractive indexes are essentially different from the average values that can be predicted in the simple model of an effective dielectric medium. Filling pores with dielectric liquid induces a dramatic modification of the optical properties of the structures.

1. Introduction

Nanocomposite materials are a subject which recently started to attract great interest of researchers. The materials are artificial ones that are made of several nanosize components fused into a quasi-crystalline structure. Properties of such materials are very different from those of components [1]. Nanocomposites can be used for manufacturing new materials with novel electrical, optical, mechanical and other properties. Among different nanocomposites an important role is played by porous semiconductors and dielectrics with nanometer-scale pore size. The very large surface in porous semiconductors allows one to use them as sensors of gases and liquids [2,3].

The best results were achieved for the porous alumina [4,5] and silicon [6–8] that find applications in optoelectronics and as a catalyzer for monoatomic oxygen synthesis. Results in fabrication and study of A2B6 and A3B5 semiconductors have been rather modest [9–11]. The main problem lies in the synthesis of porous matrices with controllable sizes, homogeneity and pore direction.

The most promising results in obtaining extremely uniform arrays have been obtained for porous silicon [12,13]. Optical properties of these structures were studied in Ref. [14].

In this paper we report on fabrication and characterization of a homogeneous array of nanopores in InP structures aligned along the [1 0 0] and [1 1 1] directions, respectively.

2. Experiment

Two sets of nanoporous InP samples have been prepared. In set #1 pores are aligned along the [1 0 0] direction. In set #2 there is a 8.5 μm transition layer with pores directed along the [1 1 1] direction. The samples were fabricated by anodic electrochemical etching of industrial *n*-type [1 0 0] InP substrates ($\sim 2\times10^{18}$ cm^{-2} for set #1 and $\sim 8\times10^{17}$ cm^{-2} for set #2, respectively) in aqueous chloride electrolyte [15]. The pore formation is carried out according to a reaction of nucleophilic substitution [16]. Choosing the current-pulse parameters, composition, and concentration of the electrolyte and substrate doping level enables to control the direction, width, and deepness of the pores [17,18].

As a result, one obtains a nanoporous semiconductor material with a system of square pores with an average width from 20 to 70 nm and length up to $\sim$150 μm. The aspect ratio (length/width) reaches 7500. Pore-width dispersion does not exceed 15%. Pore-length uniformity is controlled by homogeneity of the impurity distribution in the InP substrate. There is an irregular transition layer with a thickness 2 μm near the surface of the samples. After finishing the etching, the porous layer is separated from the substrate by change of the etching regime. Morphological and optical investigations were carried out for both types of samples.

Fig. 1 presents an image of a sample from set #1 in the direction [1 0 0], perpendicular to the sample surface obtained by Scanning Electron Microscope (SEM). This sample contains a 30 μm-thick layer of pores in the [1 0 0] direction. The coefficient of porosity for this sample is $\sim$70%, the average size of the pores is 50 nm, the size dispersion is 15%, and the thickness of the pore walls is 13–15 nm.

Fig. 2 presents an SEM image of a sample from set #2 taken in the direction [1 1 0]. In the sample the near-surface layer has pores aligned in the direction [1 1 1]. The sample contains a 8.5 μm-thick micron transition layer of pores in the [1 1 1] direction and a 25 μm-thick layer of pores in the [1 0 0] direction. The coefficient of porosity is $\sim$70%, the pore size is 55 nm, the dispersion of the size is 17%, and the thickness of the pore walls is 13–18 nm.

Absorption spectra of all the samples near the fundamental absorption edge are practically identical. An absorption spectrum

* Corresponding author at: Ioffe Physical-Technical Institute, Russian Academy of Sciences, Politekhnicheskaya ul. 26, St. Petersburg 194021, Russia.
E-mail address: vladimir.kochereshko@mail.ioffe.ru (V.P. Kochereshko).

1386-9477/$ - see front matter © 2012 Elsevier B.V. All rights reserved.
doi:10.1016/j.physe.2012.02.012

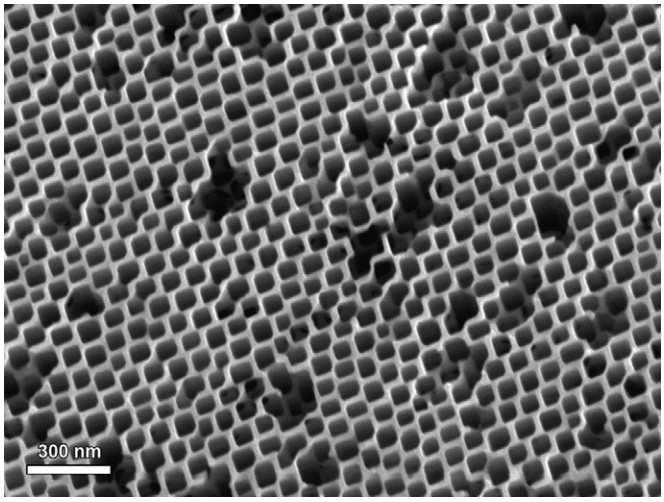

Fig. 1. Scanning Electron Microscopy image of the surface of a porous InP sample from set #1. In the sample pores are aligned along the [1 0 0] direction. The scale is shown by white piece of a line.

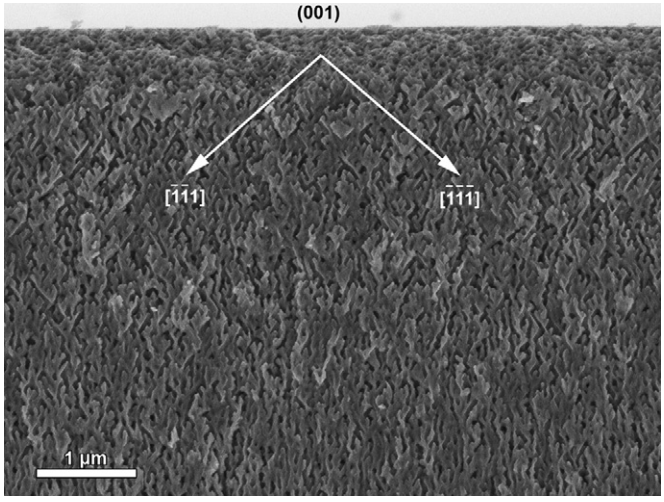

Fig. 2. Scanning Electron Microscopy image of a cross section of a porous InP sample from set #2. Pores in the sample are aligned along the [1 1 1] direction in the plane of the (1 $\bar{1}$ 0)

of a porous sample from set #1 is compared with a spectrum of a bulk InP sample in Fig. 2. One can see that the absorption edge of the porous sample is extended to low energies. This is an indication that the electron and hole states at the band edges form tails of localized states, which is typical for non-ordered (non-crystalline) structures. Indeed, in our samples there is a notable distribution of wall thickness from 13 nm to 15 nm. The distribution of electron and hole quantized energies in the walls leads to the spread of the effective band-edge.

Because the size of the pores is smaller than the light wavelength we consider the structures as a homogeneous continuous medium with an effective dielectric function (*we neglect here the interferences of the light reflected from different layers in the structure*). There are numerous theoretical models to describe the dielectric function of nanocomposite materials [1]. Regardless to any model we should expect that the dielectric function for the light polarized along pores ($\varepsilon_{eff}^{\parallel}$) and perpendicular to pores ($\varepsilon_{eff}^{\perp}$) are different and $\varepsilon_{eff}^{\parallel} > \varepsilon_{eff}^{\perp}$.

Below band-edge transmission spectra for linearly and circularly polarized light were measured at normal and oblique incidence from these structures. The linear polarizer was always oriented along a direction at 45° with respect to the vertical axis. We used a linear analyzer to measure the degree of linear polarization in the direction that coincides with the axis of the polarizer and is revolved on 45° in respect to it. To measure the circular polarization we used a quarter wave plate. Stokes parameters of the transmitted light in the spectral range close below the band-edge have been measured.

A weak Fabry–Perot interference structure was observed below the band-edge of our samples (see inset to Fig. 3). At oblique light incidence the interference features in *S* and *P* linear polarizations do not coincide. We have used this interference structure at the incidence angle of 45° to measure the effective refractive index for the light polarized perpendicular ($n_{eff}^{\perp}$) and parallel to the pores ($n_{eff}^{\parallel}$), respectively.

We use a simple relation to determine refractive indexes from the interference structure.

$$n = \frac{\lambda_1 \lambda_2}{\lambda_1 + \lambda_2} \frac{1}{l}.$$

Here n is the refractive index, λ_1 and λ_2 are two wavelengths corresponding to neighbor maxima in the interference structure and l is the thickness of the sample.

The obtained values of the refractive indexes refer to the main axes. The data for several energies are presented in Table 1.

It should be mentioned that the values are significantly larger that it could be expected in the simple model of an effective medium. Indeed, the refractive index of bulk InP at energy 0.95 eV is $n=3.18$ [19], and the porosity of our samples is 70%. Consequently, the maximal expected value for the refractive index of a porous structure should be of the order of $n \propto 1$. This discrepancy indicates that the simple model of the refractive index averaging is not valid in our case. Nevertheless we believe that, because the

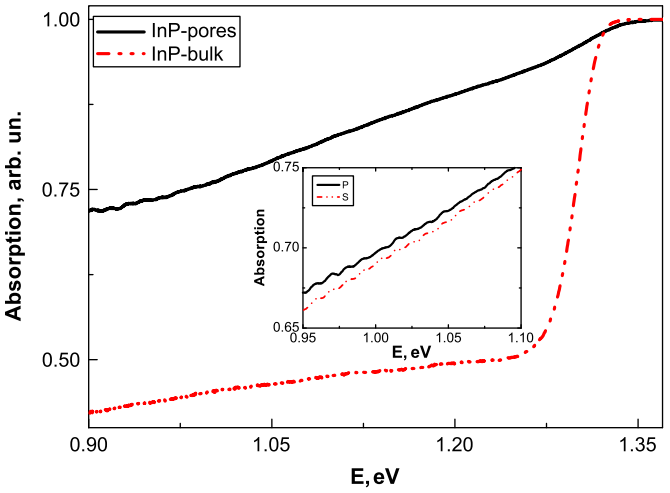

Fig. 3. Normalized absorption spectra for a porous sample with thickness of 30 μm (solid line) and normal bulk InP sample (dash dot line) 290 μm thick. The insert shows the spectrum around 1.0 eV where the Fabry–Perot interference is better visible.

Table 1
Refractive indexes for the light polarized parallel and perpendicular to the pores.

Energy (eV)	$n_{eff}^{\parallel}$	$n_{eff}^{\perp}$
1.12	2.88	2.73
0.95	2.81	2.70
0.83	2.78	2.70

Please cite this article as: A.V. Atrashchenko, et al., Physica E (2012), doi:10.1016/j.physe.2012.02.012

wall thicknesses and the width of pores are less than the light wavelength, the problem is related to the method of averaging but not to the concept of the effective dielectric media. Indeed, using the model of the effective dielectric media we in fact neglect the interference effects in the structure.

When the light propagates in an anisotropic medium there are three reasons for the change of light polarization: (i) rotation of the linearly polarized light (gyrotropy), (ii) transformation of linear polarization into circular one (birefringence), and (iii) both effects together. To describe polarization properties of the light transmitted through the sample the Stokes parameters are used [20]. The Stokes parameters are the followings:

(1) Degree of linear polarization in an (X,Y) axes:

$$P_{lin} = \frac{I_X - I_Y}{I_X + I_Y},$$

where $I_{X,Y}$ is the intensity of the light that has passed through the sample and polarized in X and Y directions.

(2) Degree of circular polarization:

$$P_{circ} = \frac{I_+ - I_-}{I_+ + I_-},$$

where $I_\pm$ is the intensity of the light in right and left circular polarizations.

(3) Degree of linear polarization with respect to the axes revolved by 45° in relation to the X and Y axes around Z axis:

$$P_{lin}^{45} = \frac{I_{+45} - I_{-45}}{I_{+45} + I_{-45}}.$$

The parameters describe completely the polarization of the light. For completely polarized light: $(P_{lin})^2 + (P_{circ})^2 + (P_{lin}^{45})^2 = 1$. For partially polarized light the difference between unity and this value describes the nonpolarized component.

In our experiments we have measured these parameters at normal incidence and at oblique incidence of 45°.

3. Discussion

From the experimental data we have found no gyrotropy in all our samples, i.e. no rotation of linear polarization of light. At normal incidence no modification of the polarization of the transmitted light has been observed for the samples from set #1 (see Fig. 4).

For set #1 the sum of the Stokes parameters decreases from 95% at energy 1.1 eV to 60% at energy 0.77 eV. This depolarization indicates an increase of the light scattering efficiency by inhomogeneity of the structure. The size of the inhomogeneities is smaller than the light wavelength for the long waves and the samples are rather optically homogeneous in this spectral range. For the short wavelengths the size of the inhomogeneities is comparable to the wavelength. As a result, the efficiency of the Rayleigh scattering and depolarization is higher for the short wavelength.

At oblique incidence Fig. 5 we found a transformation of the linear polarization into the circular one, which means birefringence. Indeed, the refractive indexes along and perpendicular to the pores, respectively, are different and consequently birefringence effect appears. From these data we also can estimate the difference of the refractive indexes $(n_{eff}^{\parallel} - n_{eff}^{\perp})$, which is found to be very close to that we obtained from the interference structure.

In the samples from set #2, we observed strong birefringence appearing even at normal light incidence, whereas birefringence was absent in samples of set #1. Contrary to the samples of set #1, in the sample set #2 there is a 8.5 μm-thick transition layer of pores aligned along the [1 1 1] direction. This layer induces birefringence at normal light incidence.

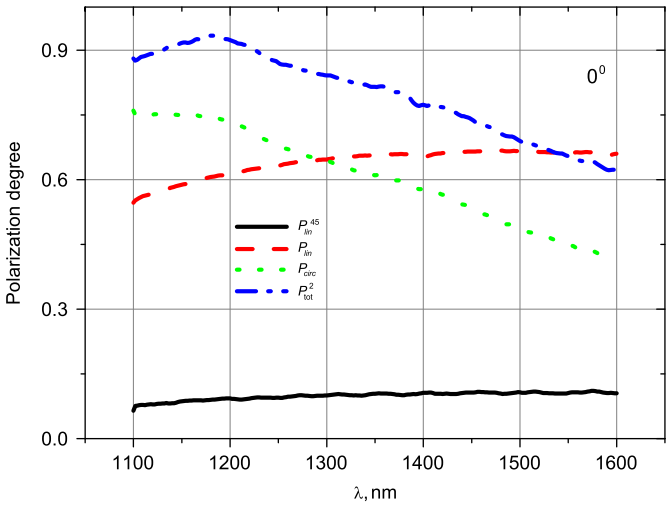

Fig. 4. Spectral dependencies of Stokes parameters: degree of linear polarization in (X,Y) axes P_{lin} (dash line), degree of linear polarization in the axes rotated by 45° with respect to the X and Y P_{lin}^{45} (solid line), degree of circular polarization P_{circ} (dot line) and sum of the squared Stokes parameters P_{tot}^2 (dash dot line) at normal light incidence.

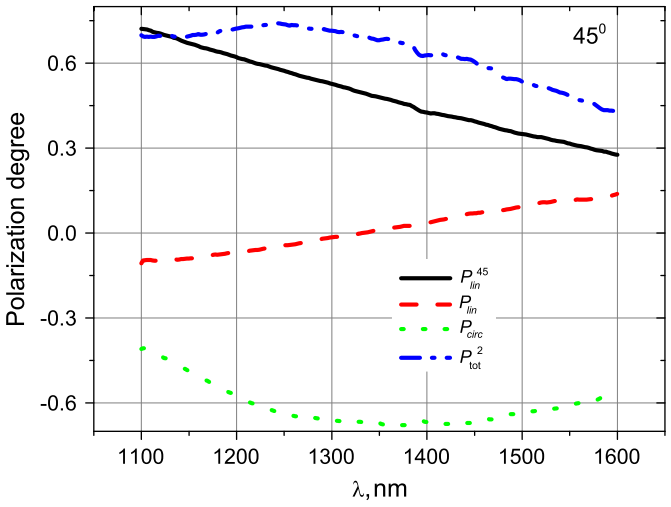

Fig. 5. Spectral dependencies of Stokes parameters: degree of linear polarization in (X,Y) axes P_{lin} (dash line), degree of linear polarization in the axes rotated by 45° with respect to the X and Y P_{lin}^{45} (solid line), degree of circular polarization P_{circ} (dot line) and sum of the squared Stokes parameters (dash dot line) at oblique incidence.

In the samples from set #2 the pores are aligned along the four crystallographically equivalent crystallographic directions [1 1 1], $[\bar{1}\ 1\ 1]$,$[1\ \bar{1}\ 1]$,$[1\ 1\ \bar{1}]$. If the pores in these directions would be exactly identical, the sample should be optically isotropic. The SEM images allow concluding only that the pores do exist but no drawing conclusions concerning their sizes. The birefringence effect indicates that the pore sizes (cross section and length) can be different for different crystallographic directions. As a result, we obtain an effective single-axis medium, in which refractive indexes for light propagating in different directions are different.

The experimental conditions for the samples from set #2 were the following. The light passed through a polarizer perpendicular

Please cite this article as: A.V. Atrashchenko, et al., Physica E (2012), doi:10.1016/j.physe.2012.02.012

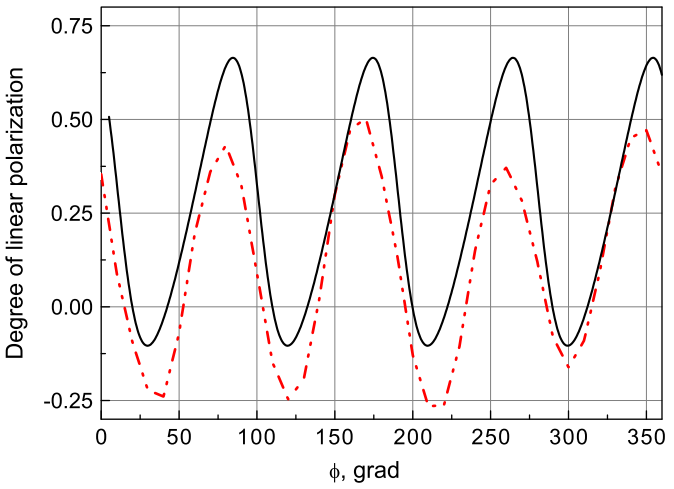

Fig. 6. Experimentally measured (dash dot line) angular dependences of the degree of linear polarization of the linearly polarized light transmitting through the sample from set #2. Calculated angular dependence according to Eq. (1) (solid line). A weak discrepancy is explained by slight nonequivalence of our polarizers. (For interpretation of the references to color in this figure legend, the reader is referred to the web version of this article.)

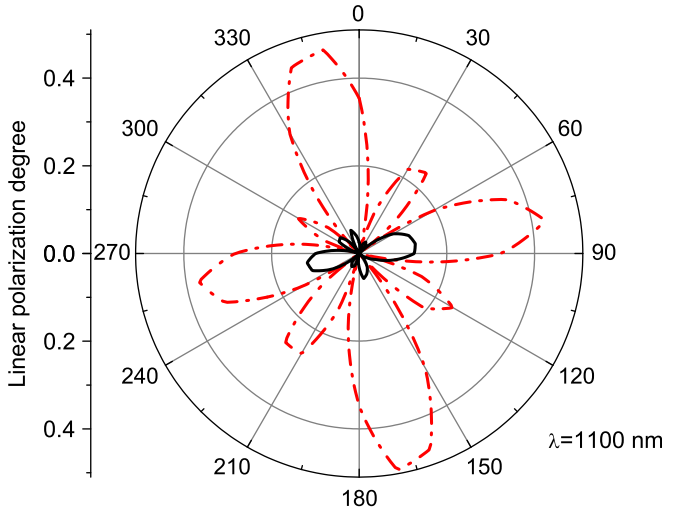

Fig. 7. Degree of linear polarization of the linear polarized light after transmitting through the sample from set #2 in polar coordinates. Dash line corresponds to the empty pores, solid line corresponds to the pores filled by $C_{10}H_7Br$.

to the sample surface. The degree of linear polarization of the transmitted light was analyzed in the axes revolved by 45° from the axis of the polarizer. The red curve in Fig. 6 shows the experimental dependence of the degree of linear polarization on the angle between the polarizer axis and the sample axis. It is seen in the figure that mainly the fourth harmonic is present in this dependence.

For the degree of polarization of linearly polarized light passing through the single-axis sample, we can derive the formula:

$$P_{circ}(\phi) = \frac{(\sin 4\phi - 2\sin^2 2\phi)\sin^2(d/2)}{2+(\sin 4\phi + 2\sin^2 2\phi)\sin^2(d/2)}. \quad (1)$$

Here ϕ is the angle between the polarization axis and the sample axis, $d = (2\pi/\lambda)\Delta n \cdot l$ is the optical thickness of the sample at the wavelength λ, l is the geometrical thickness of the sample, and Δn is the difference of the refractive indexes along and perpendicular to the pores, respectively.

The black line in Fig. 6 shows degree of polarization value calculated with following parameters: $\Delta n = 0.1$, $l = 8.5$ μm. One can see a good agreement between the theory and experiment.

We also measured such dependence for the set of samples # 2, with pores filled with dielectric liquid. As liquid we used (α)-*bromonaphthalene* ($C_{10}H_7Br$) with a refractive index $n = 1.7$ at the wavelength of 1100 nm [21]. Fig. 7 shows a comparison of the angular dependence of the degree of polarization for the sample with empty pores and for that filled with the liquid. One can see that for the filled sample the birefringence is much weaker. As a next step we plan for it to fill the pores with metal to achieve negative refraction.

4. Conclusion

Nanoporous structures based on InP semiconductors have been fabricated and studied by Scanning Electron Microscopy and by optical methods. SEM and optical measurements show that we obtained homogeneous arrays of nanopores aligned along [1 0 0] or [1 1 1] directions inside an InP matrix of 50 nm diameter and 30 μm length. Optical measurements of light polarization parameters (Stokes parameters) allow establishing the following results: (1) The structures can be considered as optically homogeneous media with an effective refractive index. (2) In the structures with [1 0 0] pore alignment, birefringence has been observed at oblique incidence. (3) Anisotropy of the refractive indexes along and perpendicular to the pores, respectively, has been measured. (4) In the structure with [1 1 1] pores alignment, birefringence has been observed at normal incidence. (5) Filling of the pores with a dielectric liquid leads to a dramatic modification of optical properties of the structures.

Acknowledgment

This work was supported in part by a grant of the Presidium PAS, POLALIS, NATO grant CLG 983878, and the state contracts 14.740.11.0270 and 14.740.11.1232 of the Ministry of Education and Science of Russian Federation. We thank also Andrey Stashkevich for very helpful discussions.

References

[1] L.A. Golovan, V.Y. Timoshenko, P.K. Kashkarov, Physics Uspekhi 50 (2007) 595.
[2] A. Foucaran, F. Pascal-Delannoy, A. Giani, A. Sackda, P. Combette, A. Boyer, Thin Solid Films 297 (1997) 317.
[3] H. Arrand, T. Benson, A. Loni, R. Arens-Fischer, M. Kruger, M. Thonissen, H. Luth, S. Kershaw, IEEE Photonics Technology Letters 10 (1998) 1467.
[4] H. Asoh, K. Nishio, M. Nakao, T. Tamamura, H. Masuda, Journal of the Electrochemical Society 148 (2001) B152.
[5] Y. Yang, Q. Gao, Physics Letters A 333 (2004) 328.
[6] D. Kovalev, H. Heckler, G. Polisski, F. Koch, Physica Status Solidi B: Basic Research 215 (1999) 871.
[7] A.A. Lapkin, V.M. Boddu, G.N. Aliev, B. Goller, S. Polisski, D. Kovalev, Chemical Engineering Journal 136 (2008) 331.
[8] A. Cullis, L. Canham, P. Calcott, Journal of Applied Physics 82 (1997) 909.
[9] M. Christophersen, S. Langa, J. Carstensen, I. Tiginyanu, H. Foll, in: 3rd International Conference on Porous Semiconductors: Science and Technology (PSST 2002), Tenerife, Spain, March 10–15, 2002, Physica Status Solidi A: Applied Research 197 (2003) 197.
[10] H. Foll, S. Langa, J. Carstensen, M. Christophersen, I. Tiginyanu, Advanced Materials 15 (2003) 183.
[11] I.M. Tiginyanu, V.V. Ursaki, E. Monaico, E. Foca, H. Foell, Electrochemical and Solid State Letters 10 (2007) D127.
[12] A. Birner, U. Gruning, S. Ottow, A. Schneider, F. Muller, V. Lehmann, H. Foll, U. Gosele, Physica Status Solidi (a) 165 (1998) 111.
[13] U. Gruninğ, V. Lehmann, S. Ottow, K. Busch, Applied Physics Letters 68 (1996) 747.
[14] F. Genereux, S.W. Leonard, H.M. van Driel, A. Birner, U. Gösele, Physical Review B 63 (2001) 161101.
[15] V.P. Ulin, S.G. Konnikov, Semiconductors 41 (2007) 832.
[16] V.P. Ulin, S.G. Konnikov, Semiconductors 41 (2007) 845.

[17] A.V. Atrashchenko, V.N. Katz, V.P. Ulin et al., Fabrication and optical properties of porous InP crystals; in: The Abstract Book of the 39th "Jaszowiec" International School and Conference on the Physics of Semiconductors, Institute of Physics, Polish Academy of Sciences, 2010.
[18] A.V. Atrashchenko, V.P. Ulin, V.P. Evtikhiev, The nanoporous matrices in the A3B5 materials: the mechanisms of formation and the reasons of destruction; in: The Abstract book of the 40th "Jaszowiec" International School and Conference on the Physics of Semiconductors, Institute of Physics, Polish Academy of Sciences, 2011.
[19] S. Adachi, Journal of Applied Physics 66 (1989) 6030.
[20] L.D. Landau, E.M. Lifshitz, The Classical Theory of Fields, vol. 2, Butterworth-Heinemann, Oxford, United Kingdom, 1975.
[21] C. Wohlfarth, Refractive Indices of Pure Liquids and Binary Liquid Mixtures (Supplement to III/38) in the Series: Landolt-Bürnstein, Numerical Data and Functional Relationships in Science and Technology, New Series, Group III: Condensed Matter, vol. 47, Springer-Verlag, Berlin/Heidelberg, 2008.

Please cite this article as: A.V. Atrashchenko, et al., Physica E (2012), doi:10.1016/j.physe.2012.02.012